

Decoding Algorithms for Hypergraph Subsystem Codes and Generalized Subsystem Surface Codes

Vinuta V. Gayatri, and Pradeep Kiran Sarvepalli, *Member, IEEE*

Abstract

Topological subsystem codes can combine the advantages of both topological codes and subsystem codes. Suchara et al. proposed a framework based on hypergraphs for construction of such codes. They also studied the performance of some subsystem codes. Later Bravyi et al. proposed a subsystem surface code. Building upon these works, we propose efficient decoding algorithms for large classes of subsystem codes on hypergraphs and surfaces. We also propose a construction of the subsystem surface codes that includes the code proposed by Bravyi et al. Our simulations for the subsystem code on the square octagon lattice resulted in a noise threshold of 1.75%. This is comparable to previous result of 2% by Bombin et al. who used a different algorithm.

Index Terms

quantum codes, topological codes, subsystem codes, surface codes, decoding

I. INTRODUCTION

SUBSYSTEM codes were proposed with a view to simplify quantum error correction procedures [4], [22], [23]. Subsystem codes have been studied extensively since their introduction [1], [3], [5], [7], [21], [25]–[27]. To understand how they help recall that in a typical error correction cycle we need to i) measure the syndrome, ii) estimate the error from the syndrome, and iii) apply the estimated error as correction. Subsystem codes can be beneficial in the first and last steps.

Typically, quantum codes require many body operators for measuring the syndrome. Subsystem codes can potentially simplify the syndrome measurement process by breaking down the many qubit measurement into a simpler set of measurements, where each measurement involves a fewer number of qubits. The outcomes of these measurements are combined classically to obtain the measurement of the original operator. Subsystem codes also allow for a greater degree of freedom in the correction operator. In addition, we can tolerate errors while encoding and syndrome measurement.

To fully leverage the advantages mentioned above we also need to develop efficient decoders for subsystem codes. Therefore this paper focusses on developing efficient decoders for certain classes of subsystem codes, specifically topological subsystem codes (TSCs), which are suitable for fault tolerant quantum computing.

The first construction of topological subsystem codes is due to Bombin [7]. The stabilizer generators of these codes are local, unlike the Bacon-Shor code. (Large weight stabilizers are not preferred from a fault tolerance point of view.) They are derived from color codes and are also called topological subsystem color codes (TSCCs). In these codes, the syndrome measurements can be performed by measuring two qubit operators. Furthermore, each syndrome can be reconstructed from $O(1)$ such local operators.

Suchara et al. [27] proposed a framework based on hypergraphs within which one could construct TSCCs and many other topological subsystem codes. They also proposed two step decoding algorithms for some specific subsystem codes. Using the framework of [27] many new classes of topological subsystem codes were proposed in [26]. However, no decoding algorithms were proposed for them.

While many topological subsystem codes can be constructed using the hypergraph framework, not all TSCs can be constructed within this framework. Bravyi et al. proposed a TSC outside this framework in [13]; it was called the subsystem surface code (SSC). For this code, syndrome measurements require 3-qubit measurements. This was also suitable to a 2D implementation like the planar surface code. This code was built from a square lattice and it left open the question of a more general construction of such codes.

In this paper we are concerned with the *problem of efficiently decoding topological subsystem codes from hypergraphs and generalized subsystem surface codes*. Our paper builds on results in [13], [26], [27]. First, we generalize the two step decoding algorithms of [27] to large classes of hypergraph subsystem codes. We then propose new constructions of surface subsystem codes and develop efficient decoders for them. Along the way we also prove some structural results on the hypergraph subsystem codes and subsystem surface codes.

A detailed summary of our contributions is as follows:

- (i) For the cubic subsystem codes derived (from color codes) we propose a one step decoding algorithm which we call the colored matching algorithm.

Vinuta V. Gayatri is currently with Madstreet Den Technologies Pvt Ltd., Bangalore, India.

Pradeep Kiran Sarvepalli is with Department of Electrical Engineering, Indian Institute of Technology Madras, India.

- (ii) We show that the TSCCs can be decoded in a two step process, where the bit flip errors are corrected first and the phase flip errors are corrected by mapping them to a color code. This is built on the observation in [27] about the subsystem code on square octagon lattice. We decode this code using this method and show that it has a threshold of 1.75% which is comparable to the threshold of 2% obtained by [9] who used a renormalization group decoder algorithm.
- (iii) We then study decoding algorithms for a class of quantum codes which generalize the five-squares subsystem code proposed in [27]. Unlike the previous class of codes the decoding of these codes leads to a mapping on two copies of a surface code. We identify explicitly the surface codes onto which the subsystem codes are mapped.
- (iv) We propose a new construction for subsystem surface codes. For all these codes, syndrome can be extracted by means of three-qubit measurements. Using this construction we obtain a family of subsystem codes with lower overhead than the codes proposed in [13].
- (v) We show that the proposed subsystem surface codes can be decoded by mapping to a pair of surface codes. This result generalizes the algorithm of [13] to the proposed subsystem surface codes.

The rest of the work is organized as follows: In section II, there are basic mathematical preliminaries and the constructions of subsystem codes required to understand the decoding algorithms we have proposed. In section III, we present two algorithms to decode cubic subsystem color codes. In sections IV, V and VI, we present different decoding algorithms for topological subsystem color codes, generalized five squares subsystem codes and subsystem surface codes, respectively. In section VII, the simulation results for the subsystem code on the square octagon lattice are given. We conclude in section VIII.

II. BACKGROUND

A. Mathematical preliminaries

In this section, we present a brief review of some graph theoretic concepts which we use in the discussions to follow.

A graph Γ is an ordered pair $(V(\Gamma), E(\Gamma))$ where $V(\Gamma)$ is a set of vertices in Γ and $E(\Gamma)$ is a set of edges in Γ . If there are m edges incident on a vertex v , then v is said to have a degree of m . A face in a graph is a region bounded by edges.

A path is a sequence of vertices (v_1, v_2, \dots, v_k) where there exists an edge (v_i, v_{i+1}) for all $i \in 1, 2, \dots, k-1$ and all vertices are distinct except possibly v_1 and v_k . A graph is called a connected graph if there exists a path between each pair of vertices. A closed path in a graph is called a cycle. That is, in the path (v_1, v_2, \dots, v_k) if $v_1 = v_k$, then it is a cycle. A cycle σ is also represented by an ordered set of edges (e_1, e_2, \dots, e_k) . Every vertex in a cycle has an even degree with respect to the edges in the cycle.

For a graph Γ with a set of vertices $V(\Gamma)$ and set of edges $E(\Gamma)$, a matching is a subgraph of Γ such that there is at most one edge incident on each vertex $v \in V(\Gamma)$. In other words, no two edges in the matching share a common vertex. Perfect matching is a matching where there is exactly one edge incident on every vertex. A weighted graph is a graph where each edge is associated with a weight which is, in general, a positive number. Cost of a matching in a weighted graph is the sum of the weights of the edges of the matching. Minimum weight matching is the matching such that it has the lowest cost among all the possible matchings.

The dual of a graph Γ embedded on a surface is a graph which has a vertex for every face in Γ and an edge between two vertices if the corresponding faces on Γ are adjacent. The dual of Γ is denoted as Γ^* .

The medial graph of a graph Γ is defined as a graph which has a vertex for each edge in Γ and an edge between two such vertices if the corresponding edges in Γ are incident on the same vertex in Γ . We denote the medial graph of Γ by Γ_m .

A hypergraph \mathcal{H} is two-tuple $(V(\mathcal{H}), E(\mathcal{H}))$, where $V(\mathcal{H})$ is the vertex set and $E(\mathcal{H})$ is the collection of edges. An edge e is a subset of $V(\mathcal{H})$. An edge with two vertices is called a simple edge and the one with more than two vertices is called a hyperedge. If $e = (u_1, u_2, \dots, u_k)$ we say it is a rank- k edge and e is said to be incident on u_i for $1 \leq i \leq k$. In this paper we restrict our attention to edges of rank two or three.

A hypercycle σ is a collection of edges in a hypergraph such that every vertex in the support of the edges has an even degree with respect to the edges. Figure 1 shows cycles in a hypergraph.

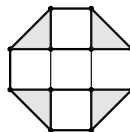


Fig. 1: A rank-3 hypergraph: The gray triangles are the hyperedges of the graph. The four inner rank-2 edges form a rank-2 cycle while the hyperedges along with the bold edges form a hypercycle.

We denote the vertices, edges of the graph Γ by $V(\Gamma)$, $E(\Gamma)$ while the faces of the embedding of Γ are denoted by $F(\Gamma)$. Also $F_c(\Gamma)$ and $E_c(\Gamma)$ denote the set of all c -colored faces and c -colored edges respectively. If Γ is a cubic graph such that the faces are 3-colorable, then it is called a 2-colex. In a 2-colex, the edge colouring is induced by the faces. An edge connecting c -colored faces is also c -colored. In the dual graph Γ^* , the set of vertices corresponding to c -colored faces of Γ is denoted by $V_c(\Gamma^*)$.



Fig. 2: (Color online) Relations among groups related to stabilizer codes and subsystem codes

B. Stabilizer codes and subsystem codes

1) *Stabilizer Codes*: We quickly review the stabilizer formalism, see [14], [16], [17] for more details. Denote by \mathbb{P}_n the Pauli group on n qubits. Let S be a commutative subgroup of \mathbb{P}_n , such that $-I \notin S$. The stabilizer code defined by S is the joint +1-eigenspace of S ; Mathematically, it can be written as,

$$S = \{h \in \mathbb{P}_n \mid h|\psi\rangle = |\psi\rangle \text{ for all } |\psi\rangle \in Q\}$$

S is called the stabilizer of Q . An $[[n, k]]$ stabilizer code encodes k qubits into n qubits and it is completely characterized by $n - k$ independent stabilizer generators. The measurement outcome of the stabilizer generators is called the syndrome. If there is a nontrivial syndrome, it indicates the presence of an error.

The centralizer of S , denoted $C(S)$, is defined as

$$C(S) = \{h \in \mathbb{P}_n \mid gh = hg \text{ for all } g \in S\}$$

Since the elements of S act trivially on the elements of Q , errors in $\langle iI, S \rangle$ are harmless. If the error operator is not an element of $C(S)$, then the error can be detected. An element of $C(S)$, but not an element of $\langle iI, S \rangle$, acts like a logical error and cannot be detected. (These relations are summarized in Fig. 2.)

The weight of a Pauli error g is defined as the number of qubits on which it acts nontrivially and denoted $\text{wt}(g)$. An $[[n, k]]$ quantum code is said to have distance d where

$$d = \min\{\text{wt}(e) \mid e \in C(S) \setminus \langle iI, S \rangle\}. \quad (1)$$

An $[[n, k, d]]$ code can detect all errors with weight up to $d - 1$.

Suppose an error $e \in \mathbb{P}_n$ occurs on the code space. When we measure the stabilizer generator $g \in S$, it results in the syndrome $s \in \{0, 1\}$ where $ge = (-1)^s eg$.

2) *Subsystem codes*: We review subsystem codes briefly, see [3], [4], [25] for an introduction. Let \mathcal{G} be a subgroup of the n qubit Pauli group and $C(\mathcal{G})$ the centralizer of \mathcal{G} . Let S be a (maximal) subgroup of $C(\mathcal{G}) \cap \mathcal{G}$ such that $-I \notin S$. Then the subsystem code defined by \mathcal{G} is +1-eigenspace of S . The group \mathcal{G} is said to be the gauge group of the subsystem code and elements of \mathcal{G} gauge operators. Errors in \mathcal{G} are considered to be harmless. Errors outside $C(S)$ are detectable while errors in $C(S) \setminus \mathcal{G}$ are undetectable. Suppose that \mathcal{G} and S have $2r + s$ and s generators respectively. Then \mathcal{G} defines an $[[n, k, r, d]]$ subsystem code that encodes $k = n - r - s$ qubits into n qubits and has distance d where

$$d = \min\{\text{wt}(e) \mid e \in C(S) \setminus \mathcal{G}\} \quad (2)$$

If $k = 0$, then $d = \min\{\text{wt}(e) \mid e \in \mathcal{G}, e \neq \lambda I\}$. We say the code has r gauge qubits. The subsystem code can detect all errors up to $d - 1$ qubits. (The relations between \mathcal{G} and related groups are summarized in Fig. 2.)

C. Topological codes

In this paper we are interested in a class of quantum codes called topological codes [19], see also [8] for an introduction. Of particular relevance are the families of surface codes [19] and color codes [10]. We review them briefly.



(a) Surface code on a square lattice. Qubits are on edges. Stabilizer generators A_v and B_f are defined as in Eq. (3). (b) (Color online) Color code on a hexagonal lattice. Qubits are on vertices. Stabilizer generators B_f^X and B_f^Z are defined as in Eq. (4).

Fig. 3: Topological codes

1) *Surface codes.*: Let Γ be a graph embedded on a closed surface. Qubits are attached to the edges of Γ . We define two types of Pauli operators as follows:

$$A_v = \prod_{e \in \delta v} X_e \text{ and } B_f = \prod_{e \in \partial f} Z_e, \quad (3)$$

where δv is the set of edges that are incident on the vertex v and ∂f is the set of edges that form the boundary of the face f . Operators of the type A_v are called vertex operators while B_f are called plaquette operators. We define the surface code on Γ to be the stabilizer code whose stabilizer is given by

$$S(\Gamma) = \langle A_v, B_f | v \in V(\Gamma), f \in F(\Gamma) \rangle$$

If Γ has n_v vertices and n_f faces, then there are $n_v - 1$ and $n_f - 1$ independent vertex and plaquette operators in $S(\Gamma)$. A_v and B_f generators. The surface code encodes $2g$ qubits into n_e qubits, where n_e is the number of edges and g is the genus of the surface on which Γ is embedded. So it is an $[[n_e, 2g]]$ quantum code. For instance, if Γ is embedded on a torus as in Fig. 3a, it encodes two qubits corresponding to the two independent cycles of nontrivial homology.

2) *Color codes.*: A color code is defined by a trivalent graph Γ_2 which is 3-face-colorable. By convention, these colors are taken to be red, green and blue and labeled r, g and b respectively. Such a graph is also 3-edge-colorable. The edge connecting two faces of the same color, say r , is also colored with r and so on. In case of color codes, a qubit is attached to every vertex of the graph. There are two stabilizers associated with each face of this lattice as given below :

$$B_f^X = \prod_{v \in f} X_v \text{ and } B_f^Z = \prod_{v \in f} Z_v \quad (4)$$

The stabilizer for the color code is generated by B_f^X, B_f^Z for all $f \in F(\Gamma_2)$. The honeycomb lattice is an example of a color code, see Fig. 3b. A method to obtain 2-colexes is given in Construction 1.

Construction 1: Color codes from graphs [12]

Given an arbitrary graph, color each face with $x \in \{r, g, b\}$ and split each edge into two edges. Color the faces formed after splitting the edges with $y \in \{r, g, b\} \setminus x$. Then change each vertex of degree d to a face with d edges and color them with $z \in \{r, g, b\} \setminus \{x, y\}$.

Note that the 2-colex from Construction 1 has three kinds of faces: those obtained from faces, edges and vertices. They are called f -faces, e -faces and v -faces respectively. All the faces of a certain type are colored the same.

D. Subsystem codes from graphs and hypergraphs

This subsection reviews topological subsystem codes based on cubic lattices and hypergraphs. Suchara et al. proposed a framework within which we can construct subsystem codes from cubic graphs and rank-3 hypergraphs [27]. A subsystem code is constructed from a trivalent rank-3 hypergraph \mathcal{H} as follows. Qubits are placed on the vertices of \mathcal{H} . We associate to each edge of the hypergraph a Pauli operator K_e called edge operator

$$K_e = \begin{cases} g_u g_v & \text{if } (u, v) \in E_2(\mathcal{H}) \\ Z_u Z_v Z_w & \text{if } (u, v, w) \in E_3(\mathcal{H}) \end{cases} \quad (5)$$

subject to the following constraints:

$$|e \cap e'| \leq 1 \quad \text{and} \quad K_e K_{e'} = (-1)^{|e \cap e'|} K_{e'} K_e \quad (6)$$

From the hypergraph we derive a standard graph $\overline{\mathcal{H}}$ without hyperedges by promoting each hyperedge (u, v, w) to three regular edges (u, v) , (v, w) and (w, u) . This derived graph is used to define the gauge group \mathcal{G} of a subsystem code. We define the link operators \overline{K}_e as

$$\overline{K}_{u,v} = \begin{cases} K_e & \text{if } (u, v) \in E_2(\mathcal{H}) \\ Z_u Z_v & \text{if } (u, v) \subset (u, v, w) \in E_3(\mathcal{H}) \end{cases} \quad (7)$$

$$\mathcal{G} = \langle \overline{K}_{u,v} \mid (u, v) \in E_2(\overline{\mathcal{H}}) \rangle, \quad (8)$$

where \mathcal{G} is the group generated by the link operators.

The hypergraph also defines the centralizer of the gauge group, denoted by $C(\mathcal{G})$. Let σ be a hypercycle of \mathcal{H} . Then we define as the cycle operator W_σ

$$W_\sigma = \prod_{e \in \sigma} K_e \quad (9)$$

$$\text{Then } C(\mathcal{G}) = \langle W_\sigma \mid \sigma \text{ is a hypercycle of } \mathcal{H} \rangle \quad (10)$$

Using this framework we can construct many families of subsystem codes. We restrict our attention to the following families of codes within this framework.

1) *Cubic subsystem color codes* : Consider a cubic graph (that is also bipartite). We consider only the case when the graph Γ is a 2-colex. Then Γ is 3-face-colorable and 3-edge-colorable. We can assign the edge operator K_e based on the color. Without loss of generality, we assume

$$K_e = \begin{cases} X_u X_v & (u, v) \in E_x(\Gamma) \\ Y_u Y_v & (u, v) \in E_y(\Gamma) \\ Z_u Z_v & (u, v) \in E_z(\Gamma), \end{cases} \quad (11)$$

where x, y, z are three distinct colours. We have the following dependency among the edge operators of a cubic subsystem code.

$$\prod_e K_e = I \quad (12)$$

As a consequence of the above assignment, a c -colored face is bounded by an alternating sequence of edges of color $\{x, y, z\} \setminus \{c\}$ where $c \in \{x, y, z\}$. Every cycle leads to a stabilizer. Therefore, the stabilizer associated to each face is as follows.

$$B_f = \begin{cases} \prod_{v \in f} X_v & f \in F_x(\Gamma) \\ \prod_{v \in f} Y_v & f \in F_y(\Gamma) \\ \prod_{v \in f} Z_v & f \in F_z(\Gamma) \end{cases} \quad (13)$$

There are also additional stabilizer generators coming from homologically nontrivial cycles of Γ . We call these codes *cubic subsystem color codes* indicating that the underlying cubic graph is a 2-colex. We can easily show the following result about these codes.

Lemma 1 (Cubic subsystem color codes). *A 2-colex with n vertices gives rises to an $[[n, 0, n/2 - 1, 2]]$ subsystem code.*

Proof. In a 2-colex the number of edges is $e = 3n/2$. Therefore the number of linearly independent gauge generators is $3n/2 - 1$. The number of independent stabilizer generators is given by $s = f + 2g - 1$. Since $n - 3n/2 + f = 2 - 2g$, we have $f = n/2 + 2 - 2g$ and $s = n/2 + 1$. Let r be the number of gauge qubits. Then $3n/2 - 1 = 2r + s$, giving $r = n/2 - 1$ gauge qubits. The dimension of the subsystem code is $k = n - s - r = 0$. Finally the distance is two since, $\min \text{wt}(\mathcal{G}) = 2$. \square

2) *Topological subsystem color codes* : A method to construct topological subsystem codes [7] is to start with a 2-colex and perform the following sequence of operations. Expand every vertex into a triangle and split every edge into a pair of edges as shown in Fig. 4. We identify every triangle with a rank-3 edge. The resulting hypergraph is trivalent and 3-edge-colorable. We color the rank-3 edges one color say blue, and the rank-2 edges incident on every hyperedge red and green in an alternating fashion as shown in Fig. 4. An example is shown in the Fig. 5. Then we can assign the link operators as in Eq. (11).

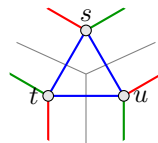


Fig. 4: (Color online) A vertex of the 2-colex along with its incident edges is shown (grey) and the subsequent vertex expansion shown in color. The rank-3 edge is always coloured blue. The rank-2 edges are coloured with red (solid) and green in an alternating fashion going clockwise around a rank-3 edge.

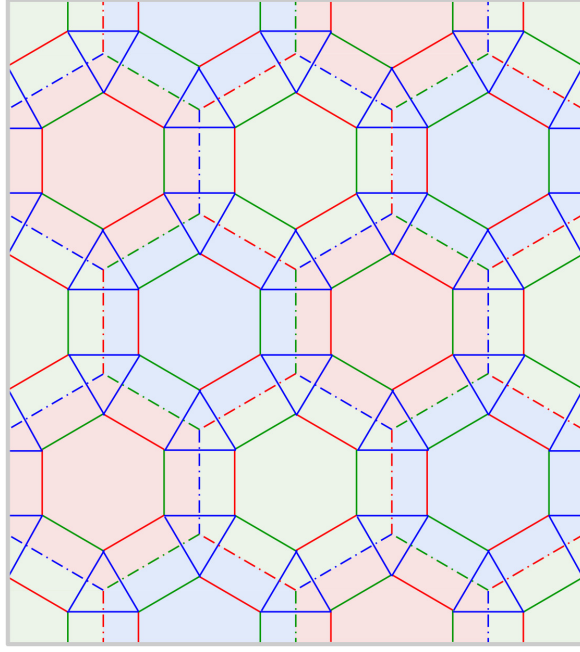


Fig. 5: (Color online) Illustrating vertex expansion on the hexagonal lattice.

In the hypergraph generated from the 2-colex by vertex expansion, we can associate two independent cycles for each face: i) one rank-2 cycle and ii) one hypercycle. Therefore we obtain two independent stabilizer generators for each face. The cycles lead to the following stabilizer generators.

$$W_1^f = \prod_{v \in f} Z_v \quad (14)$$

$$W_2^f = \prod_{(u_i, v_i, w_i) \in f} X_{u_i} Y_{v_i} Y_{w_i} \quad (15)$$

The codes obtained from this construction have the following parameters.

Lemma 2 (Topological subsystem color codes [7]). *A 2-colex Γ , embedded on a surface of genus g , on vertex expansion leads to a $[[3n, 2g, 2n + 2g - 2, d \geq \ell]]$ subsystem code, where n is the number of vertices in the 2-colex and ℓ is the length of the smallest cycle of nontrivial homology in Γ .*

3) *Hypergraph subsystem codes*: Another class of subsystem codes were proposed in [26] using the framework of Bravyi et al. They are also based on color codes. The central idea behind the constructions of [26] is to come up with a trivalent, 3-edge colorable hypergraph by promoting some of the edges of a 2-colex to rank-3 edges. On promoting some rank-2 edge to rank-3 edges the resulting graph is not necessarily trivalent, so additional rank-2 edges are added to make for those vertices that are deficient in degree. Since the 2-colex is 3-edge colorable, with a little care we can ensure that the resulting hypergraph is also 3-edge-colorable.

Construction 2: Hypergraph subsystem codes from color codes [26]

Given a 2-colex Γ_2 and a subset of r -colored faces $F \subseteq F_r(\Gamma_2)$ such that $|f| \equiv 0 \pmod{4}$ and $|f| > 4$ for all $f \in F$. Inside each $f \in F$, add a face f' such that f' has $|f|/2$ edges. Take an alternating set of edges in the boundary of f and promote them to hyperedges such that (i) the third vertex of a hyperedge comes from the face f' and (ii) the hyperedges do not cross each other.

We consider two families of hypergraph subsystem codes:

- i) $F = F_r(\Gamma_2)$
- ii) $F \subsetneq F_r(\Gamma_2)$

We call the codes from first choice as uniform rank-3 hypergraph subsystem codes and the codes from the latter as generalized five-squares subsystem codes. These codes are explored in Sections. IV and V respectively.

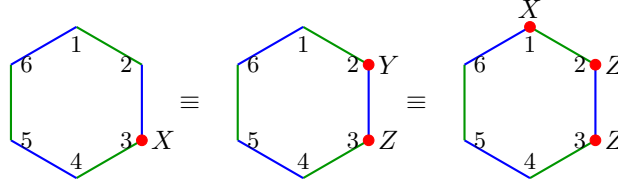


Fig. 6: (Color online) The green edges represent XX operators and the blue edges represent YY operators. Thus X error on qubit 3 of the hexagonal face, ie. X_3 is equivalent to Y_2Z_3 , which is in turn equivalent to $X_1Z_2Z_3$.

III. DECODING CUBIC SUBSYSTEM COLOR CODES

The prototype cubic subsystem code is Kitaev's honeycomb model [20]. This was not originally viewed as a subsystem code. Suchara et al. [27] made this connection to subsystem codes clear. Although the cubic subsystem codes are $[[n, 0]]$ quantum codes, it is instructive to study them. For instance, Kells et al. [18] showed that the honeycomb model can be approximated by a toric code. Recently, Lee et al. [24] showed that the honeycomb model can be viewed as an approximate error correcting code. Suchara et al. studied the hexagonal subsystem code to obtain valuable insights into syndrome measurement using two qubit operators. These developments indicate that it is worthwhile to study cubic subsystem codes.

We restrict our attention to the cubic subsystem color codes i.e. cubic subsystem codes based on 2-colexes, see Section II for a brief review. We study the decoding of these codes and propose a number of algorithms which have natural extensions to hypergraph subsystem codes which encode a nontrivial number of logical qubits. The key ideas are much more transparent in the context of cubic subsystem codes.

A. A decoder for cubic subsystem color codes

We propose a decoding algorithm for the cubic subsystem codes. This generalises the method proposed in [27] to cubic subsystem codes. In this method all the X errors are corrected in the first step. This could introduce some new Z type errors. In the next step all the Z errors are mapped to a surface code. We then decode the errors on the surface code. The resulting error estimate (on the surface code) is then lifted to the subsystem code leading to an error estimate for the subsystem code. This completes the error correction cycle.

Two errors that differ by an element of the gauge group cannot be distinguished by the subsystem code. We consider such errors equivalent. The next lemma shows that for every error there is an equivalent error that has a structure which simplifies the error correction.

Lemma 3 (Error equivalence modulo gauge group). *An error on a cubic subsystem code is equivalent to another error which has*

- (a) *at most one X or Y error per z -face*
- (b) *Z errors on the remaining qubits*

Proof. Let Γ_2 be the 2-colex on which the cubic subsystem code is defined. The z -colored faces of Γ_2 are disjoint and cover all the vertices of Γ_2 , it suffices to show that the error on any such face is equivalent to a Z -only error. Let $f \in F_z(\Gamma_2)$. Since all faces in 2-colex have even number of edges we can assume that the link operators for the edges in the boundary of this face are given by $K_{e_1}, \dots, K_{e_{2\ell}}$ where $e_{2i} \in E_x(\Gamma_2)$ and $e_{2i+1} \in E_y(\Gamma_2)$. The product of the link operators of the first $i < 2\ell$ edges will give us

$$K_{e_1}K_{e_2} \cdots K_{e_i} = \begin{cases} X_1Z_2 \cdots Z_iX_{i+1} & i \text{ odd} \\ X_1Z_2 \cdots Z_iY_{i+1} & i \text{ even} \end{cases} \quad (16)$$

It follows from these equations that X_{i+1} is equivalent to $X_1Z_2 \cdots Z_i$ if i is odd, else X_{i+1} is equivalent to $X_1Z_2 \cdots Z_iZ_{i+1}$. Therefore, an arbitrary error can be reduced to at most one X error and a combination of Z errors on the remaining qubits. \square

Figure 6 shows an illustration of lemma 3. The blue-colored edges of the hexagon are associated with the link operator YY and green-colored edges are associated with the link operators XX . The hexagon represents a red -colored face of a 2-colex on which the subsystem code is defined. An equivalent of an error is obtained by multiplying the error with the link operator associated with an adjoining edge.

Corollary 4 (Correcting X errors up to gauge). *An X error on a cubic subsystem code can be corrected up to a gauge operator by measuring the Z -stabilizers.*

Proof. By Lemma 3, we know that every error is equivalent to an error that contains at most one X or Y error on every z -face of Γ_2 . By Eq. (13), the stabilizer associated to f is given by

$$B_f = \prod_{e \in \partial f} K_e = \prod_{v \in f} Z_v \quad (17)$$

The stabilizers of distinct z -faces have disjoint support, therefore we can correct each of the errors independently. If the stabilizer of an r -face gives a nontrivial syndrome then we can apply an X error on one of the qubits otherwise we make no correction. This process completely estimates all the X errors. \square

After correcting the bit flip errors on the cubic subsystem code we are left with only phase errors. Strictly speaking, the residual error is equivalent to a Z -only error. The Z errors affect only the syndromes measured on the x and y faces. (The stabilizers corresponding to these faces are $\prod_{v \in f} X_v$ and $\prod_{v \in f} Y_v$ respectively.) We shall show the remaining Z errors can be estimated by projecting them onto a surface code.

The stabilizers of trivial homology correspond to vertices in Γ^* . These vertices can be partitioned as $V_x(\Gamma^*)$, $V_y(\Gamma^*)$, and $V_z(\Gamma^*)$. Once the bit flip errors are corrected the nonzero syndromes can be found only on the vertices in $V_x(\Gamma^*) \cup V_y(\Gamma^*)$. So we might as well delete the vertices in $V_z(\Gamma^*)$ and consider the resulting complex. Denote by $\Gamma^{*\setminus z}$ the complex obtained by (i) taking the dual of Γ and (ii) removing all the vertices in Γ^* corresponding to z -colored faces of Γ and the edges incident on these vertices. (The same complex can also be obtained by contracting all the x and y edges of Γ and then taking the dual.)

If $e := (u, v)$ is a z -edge, then it connects two z -colored faces and there is a gauge group operator acting on the qubits sitting on u and v given by $K_e = Z_u Z_v$. Hence, a Z error on the qubit u is equivalent to a Z error on v . Therefore, it is sufficient to consider either u or v for correcting the Z errors on u, v . Further, every qubit is incident on a unique z -edge. So every Z error can be identified with a unique z -edge in Γ . A Z error on a single qubit in Γ , causes nonzero syndrome on x and y faces containing it. Equivalently, it will cause nonzero syndrome on two adjacent x and y vertices. These vertices share a z -edge. Therefore a single Z error corresponds to a z edge in Γ^* . In fact this is the same unique z -edge associated with the Z error.

Therefore, a collection of Z errors corresponds to a collection of edges in $\Gamma^{*\setminus z}$. This same collection of edges can be viewed as a set of paths and cycles in $\Gamma^{*\setminus z}$. The end points of these paths correspond to the nonzero syndromes. Decoding reduces to finding a set of paths which terminate on the vertices with nonzero syndrome. This is precisely, the problem of decoding Z errors on the toric code defined by $\Gamma^{*\setminus z}$. Thus we have shown the following result.

Theorem 5 (Projecting Z errors onto a surface code). *A Z -type error, or an equivalent error, on a cubic subsystem code can be projected to Z -type error on a toric code on $\Gamma^{*\setminus z}$.*

Once we estimate the error on the toric code on $\Gamma^{*\setminus z}$, we can lift this to an error on the subsystem code easily. An error on edge (u, v) corresponds to Z_u or the equivalent error Z_v .

After decoding on the surface code, we still might have some Z errors left over since the toric code does not detect errors which form cycles on $\Gamma^{*\setminus z}$. The cubic subsystem color code can correct even such errors (modulo the gauge group) since it has $2g$ additional stabilizer generators (of nontrivial homology). Before we can correct such errors we must compute the syndrome on the non trivial stabilizer generators after accounting for the bit flip errors and the phase flip errors as estimate from the toric code. Then the residual error has no syndrome on the trivial stabilizers and can be accounted by the nontrivial stabilizers alone. For each such stabilizer S_i we find a Z error \hat{E}_i such that \hat{E}_i has an even number of errors on every x and y face and anticommutes with just one nontrivial stabilizer. Given the syndrome (s_1, \dots, s_{2g}) we estimate the error as $\prod \hat{E}_i^{s_i}$. This completes the error correction on the cubic subsystem color code. We summarize the error correction procedure in the Algorithm 1.

We now consider an example that illustrates the complete decoding process. Consider the subsystem code on honeycomb lattice on a torus with six hexagons, see Fig. 7. This subsystem code has seven independent stabilizers : five of trivial homology and two of nontrivial homology.

$$\begin{aligned}
 S_1 &= Z_1 Z_5 Z_8 Z_{10} Z_7 Z_4 & S_2 &= Z_2 Z_6 Z_3 Z_{12} Z_9 Z_{11} \\
 S_3 &= X_2 X_6 X_9 X_{11} X_8 X_5 & S_4 &= X_1 X_4 X_3 X_{12} X_7 X_{10} \\
 S_5 &= Y_3 Y_4 Y_7 X_{12} Y_9 Y_6 & S_7 &= X_7 Z_{10} Y_8 X_{11} Z_9 Y_{12} \\
 S_6 &= Y_2 X_5 X_8 Y_{11} & &
 \end{aligned}$$

The cycles associated to stabilizer generators of nontrivial homology are shown in the Fig. 7 and 8.

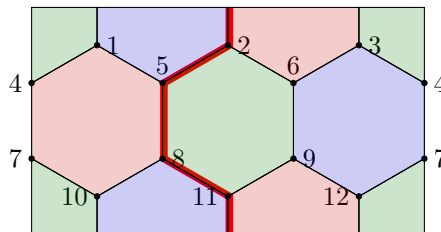


Fig. 7: (Color online) A nontrivial cycle σ_1 for a hexagonal subsystem code with 12 qubits

Algorithm 1: Decoding cubic subsystem color codes by projections

Input: A cubic subsystem code on a 2-colex Γ , syndromes on faces $s_f, f \in F(\Gamma)$ and s_i from stabilizers of nontrivial homology, $1 \leq i \leq 2g$.

Output: Error estimate \hat{E} such that \hat{E} has the input syndrome.

```

1:  $\hat{E} = I$ 
2: for  $f \in F_z(\Gamma)$  do
3:   if  $s_f \neq 0$  then
4:      $\hat{E} = \hat{E}X_v$  for some  $v \in f$  ▷ Apply correction on exactly one vertex of  $f$ 
5:     Flip the syndrome of the  $y$  face that contains  $v$ .
6:   end if
7: end for
8: Project syndromes onto  $\Gamma^* \setminus z$ 
9: Decode the errors on  $\Gamma^* \setminus z$  using any 2D toric code decoder. Denote by  $E'$ , the estimate.
10: Let  $\Omega$  be the collection edges in  $E'$ .
11: for each edge  $(u, v) \in \Omega$  do ▷ Lift the error to subsystem code
12:    $\hat{E} = \hat{E}Z_u$ 
13: end for
14: for  $1 \leq i \leq 2g$  do
15:   Let  $s'_i$  be the syndrome of  $\hat{E}$  with respect to the  $i$ th nonlocal stabilizer
16:   Update the syndrome  $s_i = s_i \oplus s'_i$ 
17: end for
18: Let  $\hat{E}_i$  be a  $Z$  error that anticommutes with all stabilizers except  $i$ th nontrivial stabilizer.
19: Return  $\hat{E} = \hat{E} \prod_i \hat{E}_i^{s_i}$ 

```

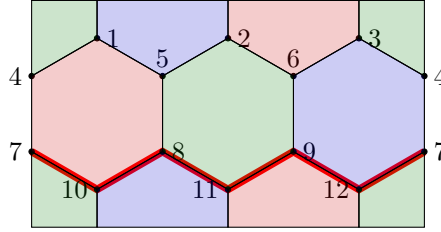


Fig. 8: (Color online) A nontrivial cycle σ_2 for a hexagonal subsystem code with 12 qubits

Suppose there is a Z -error on qubit 4 and an X -error on the qubit labeled 8, ie., $E = Z_4X_8$. Let s_i denote the syndrome for stabilizer S_i . Let the cycle associated to S_i be σ_i . We measure the following syndromes caused by this error:

$$\begin{aligned}
s_1 &= 1 & s_2 &= 0 \\
s_3 &= 0 & s_4 &= 1 \\
s_5 &= 1 \\
s_6 &= 0 & s_7 &= 1
\end{aligned}$$

We know that cycles σ_1 and σ_2 form z -faces. So we consider s_1 and s_2 to clean the X -errors. Since $s_1 = 1$, let $\hat{E} = X_1$. Remember that we can choose this X error to be on any one of the six vertices forming the cycle σ_1 . This makes s_1 equal to zero. There is no syndrome generated on the other z -face, hence we do not estimate any X -error on σ_2 . The updated syndromes are given below.

$$\begin{aligned}
s_1 &= 0 & s_2 &= 0 \\
s_3 &= 0 & s_4 &= 1 \\
s_5 &= 1 \\
s_6 &= 0 & s_7 &= 1
\end{aligned}$$

Now, we project the syndromes onto a surface code which is as shown in Figure 9 with triangular and hexagonal faces marked with black and white diagonal lines respectively. On the surface code, this set of syndromes is equivalent to the non-trivial

syndromes on two triangular faces which share a common vertex 7, and zero syndrome on all the other faces. Since the triangular faces detect Z -type syndromes, one possible error estimate on the surface code will be Z_7 . This error is equivalent to the error Z_7 or Z_{12} on the cubic subsystem code. Let us consider Z_7 . Hence the error estimate becomes $\hat{E} = X_1 Z_7$. Now the syndromes are changed to

$$\begin{aligned} s_1 &= 0 & s_2 &= 0 \\ s_3 &= 0 & s_4 &= 0 \\ s_5 &= 0 \\ s_6 &= 0 & s_7 &= 1 \end{aligned}$$

For correcting the error on the cycle σ_7 of nontrivial homology, we consider a Z -error on either qubit 7 or qubit 12. Let it be Z_{12} . To make the number of Z errors even, on the x - and y -faces on which qubit 12 resides, let us also consider Z_7 . So the final error estimate is $\hat{E} = X_1 Z_{12}$. By inspection, we see that the errors E and \hat{E} are equivalent. that is, \hat{E} is E modulo gauge group.

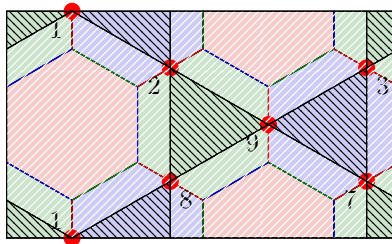


Fig. 9: (Color online) Mapping hexagonal subsystem code to surface code

B. A colored matching decoder for cubic subsystem color codes

Instead of correcting the X errors first and then correcting the Z errors by projecting onto a surface code, we could attempt to decode them simultaneously. To present this method it is helpful to view the cubic subsystem code over the dual of 2-colex. We shall first show how to represent errors in the dual complex.

Lemma 6. *Assuming the assignment of gauge operators as in Eq. (11), an X error corresponds to x -edge, Y error a y -edge and a Z error z -edge in Γ^* .*

Proof. As Γ is trivalent, every face is a triangle in the dual complex. The 3-face-colorability of Γ translates to 3-vertex colorability of Γ^* . While Γ^* is not 3-edge-colorable, we retain the coloring of edges based on Γ . Then every triangle in Γ^* is bounded by edges of three distinct colors. Further, an x -edge connects y and z vertices of each triangle. Similarly, a y -edge connects x, z vertices and z -edge connects x, y vertices.

A single qubit error can flip only two checks, therefore in Γ^* , a single qubit error leads to nonzero syndrome on just two vertices of a triangle. An X -error causes a nonzero syndrome on y and z vertices and can be identified with the x -edge connecting them. Similarly we can show that Y/Z errors can be identified with the y/z edges of the triangle. \square

By Lemma 6 we can obtain the following correspondence between edges in Γ^* and Pauli errors.

Corollary 7. *Any collection of edges in Γ^* corresponds to an error on the cubic subsystem color code.*

Note that Corollary 7 does not imply that this correspondence is unique. In fact two distinct collections of edges could correspond to the same error. For example, given any face in Γ^* , any pair of edges refer to the same error as the third edge. But these errors will be equivalent up to an element in the gauge group. Therefore, we can still refer to a collection of edges as an error, although strictly speaking it corresponds to an equivalence class of errors.

Lemma 8. *Any path in Γ^* connecting a pair of vertices u and v generates nonzero syndrome on u and v and on no other vertices. Any cycle in Γ^* generates zero syndrome. Conversely any error with nonzero syndrome on u and v alone must be a path connecting u to v up to a cycle.*

Proof. Any vertex in $V(\Gamma^*) \setminus \{u, v\}$ has an even degree with respect to the edges in the path. Therefore all checks except those associated to u and v have an even number of qubits in error. Therefore all these vertices will have zero syndrome. The checks on u and v have an odd number of errors giving rise to a nonzero syndrome. Since all vertices have an even degree with respect to the edge of cycle, all checks have zero syndrome.

The edges incident on a vertex are (single qubit) errors which anti commute with the stabilizer associated to that vertex. Hence an even degree with respect to a set of edges implies that with respect to the errors that have support on that set of

edges, the vertices in the path except at the end have zero syndromes. If an error is not a path then u (and/or v) must have even degree with respect the edges of the error. But then the syndrome would be zero on u (and/or v). Therefore it must be a path up to cycles. \square

Any path could be augmented by a cycle and it will produce the same syndrome as the path.

Lemma 9. *Any combination of errors on a cubic subsystem code will always result in an even number of nonzero syndromes.*

Proof. If there is no error then all syndromes are zero and we clearly have an even number of nonzero syndromes. Suppose that there is only one error E on qubit u where $E \in \{X, Y, Z\}$. Then u participates in the syndrome measurement of exactly three faces, f_r , f_b and f_g whose stabilizers are given by $\prod_{v \in \partial(f_r)} X_v$, $\prod_{v \in \partial(f_b)} Y_v$ and $\prod_{v \in \partial(f_g)} Z_v$ respectively. If E is an X error, then the faces f_b and f_g will have nontrivial syndromes; similarly if E is Y or Z there will be two nonzero syndromes.

Suppose that the hypothesis holds for errors up to k qubits. If there is an additional error, then the following cases can arise.

- (i) No checks are shared with other errors: The number of nonzero syndromes will increase by two.
- (ii) Exactly one check is shared: Then the check that is not shared will add one additional nonzero syndrome. The shared check could add one if it is nonzero or else it could reduce the nonzero syndromes by one if it is nonzero. In either case the nonzero syndromes are even.
- (iii) Exactly two checks are shared: If these are zero (one), then total number of nonzero syndromes will increase (decrease) by two. If only one of them is nonzero, the total number of nonzero syndromes will remain unchanged.

In all these cases the number of nonzero syndromes is even and by the principle of induction it holds for all errors on the subsystem code. \square

Corollary 10. *Error estimation from syndrome on Γ^* is equivalent to finding a collection of paths terminating on the vertices with nonzero syndromes.*

Proof. By Lemma 9 there are an even number of nonzero syndromes in Γ^* , say $2m$. We can form m pairs and each pair can be identified with a path up to cycles. This collection of paths corresponds to an error that has the given syndrome. \square

We are now ready to give the decoding algorithm.

Theorem 11 (Colored matching decoder). *The decoder given in Algorithm 2 returns the minimum weight error for a given syndrome on a cubic subsystem color code.*

Proof. The algorithm constructs a complete graph \mathcal{K} with as many vertices as there are nonzero syndromes. The edge between any two vertices in this complete graph are given by the length of the shortest path between them in Γ^* . We know that every such path corresponds to an error on Γ^* . A matching on \mathcal{K} will correspond to an error with the same syndrome as observed. A minimum weight matching will correspond to the error with the smallest weight for this syndrome. Matching in \mathcal{K} will lead to an error that has the same syndrome as observed on the stabilizers of trivial homology. To account for the syndrome on the stabilisers of nontrivial homology we need to proceed as in Algorithm 1, lines 14–19. \square

IV. DECODING TOPOLOGICAL SUBSYSTEM COLOR CODES

Topological subsystem color codes are obtained by vertex expansion of a color code. We study the decoding of these codes and their relations to surface codes. First we propose a two step decoder for the topological subsystem color codes.

Throughout this section we assume that the topological subsystem color code is built from a hypergraph \mathcal{H}_Γ which in turn is obtained by vertex expansion of a 2-colex Γ .

A. A two step decoder for topological subsystem color codes

We extend the two step decoder proposed for cubic codes to topological subsystem color codes. The basic idea is to correct X errors first and then the Z errors. The structure of the stabilizer generators then leads to a decoder that is local for X errors but global for Z errors.

Lemma 12. *An X error on a topological subsystem color code can be corrected up to a gauge operator by measuring the Z -stabilizers. The correction operator for a face f with nonzero syndrome is X_v for some $v \in f$.*

Proof. From the construction of \mathcal{H}_Γ , we see that every face in Γ gives rise to another face in \mathcal{H}_Γ . Every face of \mathcal{H}_Γ contains exactly one vertex of each rank-3 edges of \mathcal{H}_Γ . Hence, the vertices belonging to each of these faces form a partition of all the vertices in \mathcal{H}_Γ . There are two linearly independent stabilisers that we can associate to each face a rank-2 stabilizer, W_1^f and a rank-3 stabilizer, W_2^f . By Eq. (14) the rank-2 stabilizer is a Z -type stabilizer, therefore it cannot detect Z -type errors. Furthermore the qubits in W_1^f are disjoint from the qubits in $W_1^{f'}$. Therefore, if the rank-2 stabilizer of f has a nonzero syndrome, then we know that f has an odd number of X errors. An X error on any qubit of f is equivalent to an X error on

Algorithm 2: Decoding cubic subsystem color codes by colored matching

Input: A 3-colex Γ , Syndromes on vertices $s_v, v \in V(\Gamma^*)$ and s_i on stabilisers of nontrivial homology.

Output: \hat{E} with same syndrome as observed.

- 1: $\mathcal{K} :=$ complete graph on vertices u for $s_u \neq 0$
 - 2: **for** vertex v with $s_v \neq 0$ **do**
 - 3: **for** u with $s_u \neq 0$ and $u \neq v$ **do**
 - 4: Let p_{uv} be the shortest path between u and v
 - 5: $d(u, v) = \#$ edges in p_{uv}
 - 6: Form an edge between u' and v' of weight $d(u, v)$
 - 7: **end for**
 - 8: **end for**
 - 9: Find a minimum weight matching on \mathcal{K} , denote it E_m
 - 10: $P :=$ paths corresponding to E_m
 - 11: $\hat{E} :=$ error corresponding to P
 - 12: **for** $1 \leq i \leq 2g$ **do**
 - 13: Let s'_i be the syndrome of \hat{E} with respect to the i th nonlocal stabilizer
 - 14: Update the syndrome $s_i = s_i \oplus s'_i$
 - 15: **end for**
 - 16: Let \hat{E}_i be a Z error that anticommutes with all stabilizers except i th nonlocal stabilizer.
 - 17: Return $\hat{E} = \hat{E} \prod_i \hat{E}_i^{s_i}$
-

some other qubit of the face upto Z errors. Hence we can correct the X errors by simply applying a correction to each face independently of others. \square

Note that for each face f we can pick any one of its vertices to apply the error correction.

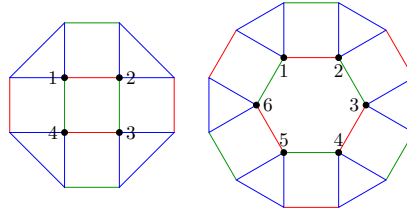


Fig. 10: Correcting X errors on subsystem codes obtained by vertex expansion. If there are an odd number of X errors then the Z type stabilizer associated with the face will register a nonzero syndrome. We can then apply a correction X_v for any one of the qubits in the face.

Once the syndromes of all the rank-2 stabilizers i.e. the Z type stabilizers are cleared, the residual error is equivalent to a Z type error. We show that these errors can be corrected by mapping onto a color code on Γ .

Let us define π to be inverse of the vertex expansion of Γ so that $\pi(\mathcal{H}_\Gamma) = \Gamma$. Let $v \in V(\Gamma)$, then we can associate to v a unique rank-3 edge $(v_1, v_2, v_3) \in E_3(\mathcal{H})$. We extend π to errors on \mathcal{H}_Γ as

$$\pi(Z_{v_1}) = \pi(Z_{v_2}) = \pi(Z_{v_3}) = Z_v \quad (18)$$

It follows that a Z error in the gauge group is mapped to identify under π . For instance, $\pi(Z_{v_1}Z_{v_2}) = I$. Let E' be an error that is equivalent to E . Then we define $\pi(E') = \pi(E)$. Finally, we project the syndrome of rank-3 stabilizers from \mathcal{H}_Γ to Γ as follows. Let s_f be the syndrome associated to the rank-3 stabilizer W_2^f .

$$\pi(s_f) = s_f \quad (19)$$

This is well defined because for every face of \mathcal{H}_Γ , we have a face in Γ .

Theorem 13 (Projecting Z errors onto a color code). *Let E be a Z -type error or an equivalent error on a subsystem code on \mathcal{H}_Γ . Then the syndrome of $\pi(E)$ is identical to the syndrome of E .*

Proof. Assume that Γ has n qubits. By Lemma 2, the subsystem code has $3n$ qubits, and subsequent to correcting the X errors we have to account for 2^{3n} phase errors. However, a Z error on any qubit of a rank-3 edge (u, v, w) are equivalent i.e. $Z_u, Z_v, Z_w, Z_uZ_vZ_w$ are equivalent errors. Thus modulo the gauge group we have to account for only 2^n phase flip errors. This is precisely the same number of phase errors on Γ .

Let $e = (v_1, v_2, v_3) \in E_3(\mathcal{H}_\Gamma)$. Then a Z error on v_i causes a nonzero syndrome on the three faces that contain the rank-3 edge. Specifically, the rank-3 stabilizers that contain e . These stabilizers are associated to three distinct faces in Γ . Now the error $\pi(Z_{v_i}) = Z_v$ has a nonzero syndrome on precisely the same faces. By linearity of π , the statement holds for all the Z type errors and errors equivalent to E since they result in the same syndrome as E . \square

An immediate consequence of Theorem 13 is that we can decode a Z type error on the subsystem color code by projecting it onto the underlying 2-colex and then lifting it back. Thus we have the following decoding algorithm.

Algorithm 3: Decoding topological subsystem color codes

Input: A substem color code on a hypergraph \mathcal{H}_Γ , where Γ is a 2-colex and syndromes $s_f^i, f \in F(\mathcal{H}_\Gamma)$ and $1 \leq i \leq 2$.

Output: Error estimate \hat{E} such that \hat{E} has the input syndrome.

```

1:  $\hat{E} = I$ 
2: for  $f \in F(\mathcal{H}_\Gamma)$  do ▷ Correct  $X$  errors locally
3:   if  $s_f^1 \neq 0$  then
4:      $\hat{E} = \hat{E}X_v$  for some  $v \in f$  ▷ Apply correction on exactly one vertex of  $f$ 
5:     Flip  $s_f^2$  and  $s_{f'}^2$ , where  $f'$  is the face adjacent to  $f$  and  $\{W_{f'}^2, X_v\} = 0$ 
6:   end if
7: end for
8: Project syndromes  $s_f^2$  onto  $\Gamma$  for all  $f \in F(\mathcal{H}_\Gamma)$  ▷ Correct  $Z$  errors globally
9: Decode the errors on  $\Gamma$  using any 2D color code decoder. Denote by  $E'$ , the estimate.
10: Let  $\Omega$  be the vertices in  $E'$ .
11: for each vertex  $v \in \Omega$  do ▷ Lift the error to subsystem code
12:    $\hat{E} = \hat{E}Z_{v_1}Z_{v_2}Z_{v_3}$  where  $(v_1, v_2, v_3)$  is the rank-3 edge associated to  $v$  ▷ It can also be lifted to  $\hat{E} = \hat{E}Z_{v_1}$  because  $Z_{v_2}Z_{v_3}$  is in gauge group.
13: end for
14: Return  $\hat{E}$ 

```

Theorem 14. *Subsystem color codes of Lemma 2 can be decoded using Algorithm 3.*

Proof. By Lemma 12 the X -type errors can be corrected locally by considering the Z type (rank-2) stabilizer generators. Following the correction some syndromes will change. Every vertex v is contained in exactly one rank-3 edge. This rank-3 edge is incident on three faces of \mathcal{H}_Γ , say f, f' and f'' . The error X_v causes non zero syndrome on exactly two rank-3 stabilizer generators: W_2^f and $W_2^{f'}$ where $v \in f$ where $\{X_v, W_{f'}^2\} = 0$ while $\{X_v, W_f^2\} = 0$. So before we can correct for the Z errors we also update the syndrome corresponding to f' . Following the correction of the X errors, the residual error is equivalent to a Z type error which by Theorem 13 can be decoded by projecting onto Γ . \square

Color codes can be (efficiently) decoded using the methods in [2], [6], [9], [15], [28], which implies that the proposed decoder is also efficient.

B. Uniform rank-3 hypergraph subsystem codes

In this section we show that the uniform rank-3 subsystem codes obtained from a bicolorable graph can also be decoded using the algorithm in the previous section. First we briefly review this construction, the reader is referred to [26] for more details.

Consider a graph Γ such that every vertex has an even degree greater than 2. Construct a 2-colex Γ_2 from Γ using construction 1. Apply construction 2 with F being the set of v -faces of Γ_2 and the hyperedges on the boundaries of e -faces of Γ_2 . Denote this hypergraph \mathcal{H} .

An illustration of this construction is given in Fig. 17. With this construction, we can define a unit cell of \mathcal{H} to be a v -face of Γ_2 along with the hyperedges and the inner face introduced by construction 2. This ensures that the support of two unit cells will not overlap and the support of all the unit cells will cover the entire lattice.

The gauge group is generated by all the link operators of $\bar{\mathcal{H}}$. Every face of \mathcal{H} gives rise to two linearly independent cycles that are homologically trivial. The associated loop operators generate the stabilizer of the subsystem code on \mathcal{H} .

We now show that these subsystem codes can also be obtained by vertex expansion but from a different 2-colex.

Theorem 15. *The uniform rank-3 hypergraph subsystem codes obtained from a bicolorable graph Γ can also be obtained from the vertex expansion of a 2-colex.*

Proof. Let Γ be a bicolorable graph, with each vertex having an even degree, from which the hypergraph \mathcal{H} representing the uniform rank-3 hypergraph subsystem code is constructed. Let Γ_2 be the intermediate 2-colex from which the hypergraph is constructed. (Refer to the section II-D.) Recall that the 2-colex from Γ has three types of faces: e -faces which are 4-sided, f -faces and v -faces. Now contract the rank-3 edges added inside the v -faces. This causes all the rank-3 edges to become vertices and the e -faces become parallel edges between two such vertices. Replace these parallel edges by a single edge. The vertices now become trivalent. The vertices of this new graph are exactly the vertices obtained from the rank-3 edges and the edges from the e -faces and the faces from the v and f -faces of Γ_2 . By assumption f -faces are bicolorable, together with the v -faces the new graph is a 3-face-colorable and trivalent. Therefore it is a 2-colex. But the operations performed are exactly the reverse of the vertex expansion operation. In other words, the subsystem code on \mathcal{H} could have been obtained by vertex expansion also. \square

From this result it follows that the uniform rank-3 subsystem codes from bicolorable graphs can be decoded by Algorithm 3.

V. GENERALIZED FIVE-SQUARES SUBSYSTEM CODES

In this section we study a generalization of the Five squares code proposed in [27]. These codes were proposed in [26, Theorem 6]. We call them nonuniform rank-3 subsystem codes. They also build on the Construction 2. Recall that there are three main ingredients to this construction. We need to pick i) a 2-colex Γ_2 ii) a collection of faces $F \subset F_r(\Gamma_2)$ and iii) edges in Γ_2 which are promoted to rank-3 edges.

Construction 3: Generalized five-squares subsystem codes [26]

Input: A bipartite graph Γ in which all the vertices have even degrees greater than 2.

Output: Subsystem code on a hypergraph \mathcal{H} .

- 1: Choice of 2-colex: Let Γ_m be the medial graph of a bicolorable graph Γ . Using construction 1 on Γ_m^* , the dual of Γ_m , obtain a three face colorable graph Γ_2 .
 - 2: Choice of F : Let the set of v -faces of Γ_2 be $F_v \cup F_f$ where F_v is the set of faces obtained from the vertices of Γ and F_f from the faces of Γ . Apply construction 2 with $F = F_v$ and let the hyperedges not be in the boundaries of the e -faces of Γ_2 .
 - 3: Choice of edges to be promoted: Outgoing edges of e -faces that also lie in F . Denote the resulting graph as \mathcal{H} and construct the subsystem code on \mathcal{H} .
-

The hypergraph obtained above is 3-edge-colorable hypergraph. We choose the following coloring scheme for the edges similar to that in [26]. This coloring can be derived from the edge coloring of the 2-colex Γ_2 . Assume that the v -faces of Γ_2 are colored red, e -faces blue and f -faces green. This implies that the e -faces which are all 4-sided must be bounded by red and green edges. Retain the edge coloring of the 2-colex whenever that edge is present in Γ_2 . Promoting the edges not in the boundaries of the e -faces implies that the edges promoted to rank-3 edges are blue. The edges of the faces newly introduced are colored red and green. We summarize this scheme directly with respect to the hypergraph as follows.

- i) Rank-3 edges are colored blue.
- ii) Unpromoted edges of faces in F are colored green.
- iii) Outgoing edges of faces in F are colored red.
- iv) Remaining edges of e -faces green.
- v) Every cycle of new rank-2 edges i.e. in \mathcal{H} but not in Γ_2 , are colored green and red in an alternating manner.
- vi) Rest of edges are colored blue.

This particular edge coloring scheme simplifies the decoding procedure we proposed for these subsystem codes. A unit cell for this graph can be a face $f \in F_v$ along with the newly introduced hyperedges and the inner face and the surrounding e -edges of Γ_2 .

The subsystem code is now defined by the resulting hyper graph. The gauge operators and the stabilizers are defined as in Section II-D. The following five types of cycles generate the stabilizer of the subsystem code, see Fig. 11. for an illustration:

- (S1) A cycle consisting of simple edges surrounding a face f where $f \in F_f$. This corresponds to stabilizer of the form $\prod_{v \in \sigma} X_v$.
- (S2) A cycle formed by alternating simple and hyperedges on the outer boundary of a face $f \in F_v$ and alternating simple edges on the boundary of its inner face introduced by construction 2. This stabilizer takes the form $\prod_{(u,v,w) \in f} X_u X_v X_w$.
- (S3) A loop consisting of simple and hyperedges around a face $f \in F_f$ which are on the boundaries of the surrounding faces. Let Ω_o and Ω_i be the qubits in the outer and inner boundary of f . Then with respect to our coloring scheme, the stabilizer can be written as $\prod_{u \in \Omega_o} Y_u \prod_{v \in \Omega_i} X_v$.
- (S4) A loop of simple edges forming the inner face of a face $f \in F_v$. This corresponds to stabilizer of the form $\prod_{v \in \sigma} Z_v$.
- (S5) A loop of simple edges forming the e -faces of Γ_2 . This corresponds to stabilizer of the form $\prod_{v \in \sigma} Z_v$.

In the following subsections an algorithm is presented to decode these subsystem codes.

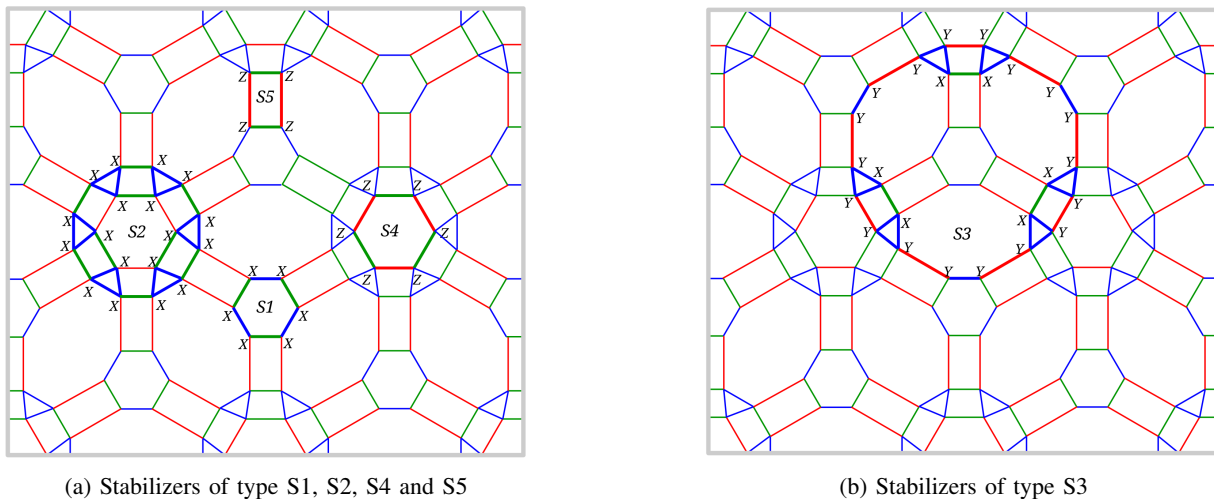


Fig. 11: (Color online) Stabilizers for nonuniform rank-3 hypergraph subsystem codes

A. Correcting X errors on generalized five-squares codes

As in the previous cases we shall first correct for the X errors on the generalized five squares codes. This is bit more complex than the algorithm for topological subsystem color codes. Let $f \in F$. Then we define a unit cell as f and the e -faces adjacent to it including the rank-3 edges and the inner face of f . Examples are shown in Fig. 12. These unit cells form a partition of the vertices (qubits) of the hypergraph. Then we can show the following result.

Lemma 16. *Bit flip errors on the generalized five-squares codes can be corrected up to a gauge operator by measuring Z only stabilizer generators. The residual error is equivalent to a Z only error.*

Proof. In each unit cell associated to a face $f \in F$, there are Z -only stabilizers associated to the e -faces and the inner face of f ie stabilizers of type (S4) and (S5) listed above. All these stabilizers have disjoint support. In each set of qubits, as we have already seen by Lemma 3, all single qubit X errors are equivalent modulo the gauge group (up to additional Z errors). So we only need to correct for one bit flip error for each of these faces. The error correction can be applied on any one designated qubit for each of the faces. \square

B. Correcting Z errors on generalized five-squares codes

After the correction of the bit flip errors modulo the gauge group, we are left with Z only errors or errors equivalent to them. Then modulo the gauge group, only a subset of qubits from each unit cell can be considered to correct the Z errors as will be shown in the following lemma.

Lemma 17. *After all the X errors are corrected on a generalized five-squares code, any combination of Z errors on a unit cell, can be reduced to one Z error for each e -face of the unit cell and exactly one Z error on one rank-3 edge as per the pattern shown in Fig. 12. The Z error on each e -face can be chosen to be on the outer boundary of the unit cell. Further, the Z error on the rank-3 edge can be corrected by measuring the stabilizer of type S2 supported on the unit cell.*

Proof. Let us consider the set of qubits on a unit cell to be a union of disjoint subsets of qubits residing on the inner face and the e -faces, say e_1, e_2, \dots, e_l when the number of edges on the inner face is l . Each e -face consists of four qubits two of which are connected to the inner face by hyperedges.

Now we make the following observations. Any set of Z errors on a rank-3 edge (u, v, w) can be reduced to identity or a single qubit Z error, say Z_u using the gauge operators $Z_u Z_v$, $Z_v Z_w$, and $Z_w Z_u$. Let us assume that this reduced error is on a qubit which is common to the rank-3 edge and an e -face. This means we have at most l such Z errors corresponding to one per rank-3 edge.

Consider a single Z error on a rank-3 edge (u, v, w) . This edge shares a vertex, say u , with an e -face. This face also shares a vertex u' with another rank-3 edge (u', v', w') . We can transfer Z error on (u, v, w) to (u', v', w') using the stabilizer of the e -face. This could add some new Z errors on the qubits of e -face which are not incident on any rank-3 edge. By repeated application of this reduction we can reduce a Z error on the rank-3 edges to a Z error pattern that is supported on exactly one qubit of one rank-3 edge and the remaining qubits of the e -faces of the unit cell.

Then, we can push one of the Z errors on any e -face to another unit cell. This is possible because the outgoing edges of the e -faces carry Z -type gauge operators. This can be done consistently for all the unit cells to obtain the pattern in Fig. 12, because these qubits belong also to the 2-colex and an inconsistent assignment will happen only if there is an odd cycle. But 2-colexes are bipartite and this is not possible.

Finally note that the stabilizer of type S2 which is supported in the unit cell is of the form $\prod_{(u,v,w) \in f} X_u X_v X_w$. It clearly anticommutes with the Z error that is supported on the rank-3 edge and can detect it. Since the other qubits do not have any support on the stabilizer, we can correct the any single qubit errors on the rank-3 edges. \square

Figure 12 shows two examples of unit cells of nonuniform rank-3 hypergraph subsystem codes with the highlighted qubits being the ones chosen for correcting the Z errors.

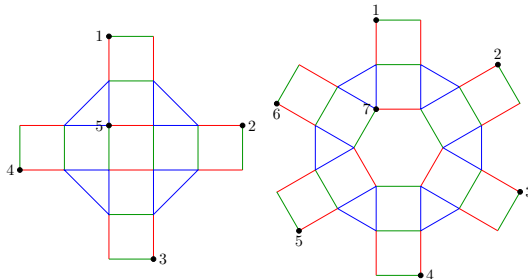


Fig. 12: Examples of Unit cells for nonuniform rank-3 hypergraph subsystem codes. The qubits highlighted are considered for Z -error corrections

It remains now to correct for the remaining Z errors on the e -faces. These errors are detected by the stabilizers of type S1 and S3. We correct these errors by mapping them onto a pair of surface codes.

Lemma 18 (Mapping to surface codes). *Consider a subsystem code constructed from Γ via Construction 3. Following the correction of X errors and errors on rank-3 edges, the residual Z errors can be corrected by mapping to a pair of surface codes.*

Proof. The residual Z -errors on each unit cell can be detected by stabilizers of type S1 and S3. Observe that any single Z error on an unit cell flips exactly one S1 type stabilizer and one S3 type stabilizer. These two stabilizers belong to two distinct faces f, f' in F_f of Γ_2 . From Construction 3, we see that these faces correspond to adjacent vertices of Γ^* . We can therefore project these syndromes to the vertices on Γ^* and the error to the edge shared by them. In this manner we obtain an error pattern on a surface code on Γ^* . (The stabilizers will be mapped to the vertex operators of Γ^* .)

Observe that if a qubit participates in the S1 type check on a face f , then it does not participate in the check of the type S3 on the same face and vice versa. Hence we can partition F_f into two subsets F_a, F_b where one set of qubits which participate in S1 stabilizers of F_a and S3 stabilizers of F_b while the other set of qubits participates in S3 stabilizers of F_a and S1 stabilizers of F_b . Thus we can project onto two copies of surfaces codes on Γ^* . \square

With these results we obtain the complete decoding algorithm for the generalized five-squares codes as given in Algorithm 4 extending the algorithm proposed for five squares codes in [27]. The proof follows by putting together all the results proved in this section. We omit the details. Efficiency of the decoding algorithm follows from the existence of efficient decoders for surface codes.

Theorem 19. *Generalized five-squares codes can be efficiently decoded using Algorithm 4.*

Fig. 13 illustrates an example of mapping the generalized five-squares subsystem code to two copies of a surface code. This is the same hypergraph subsystem code in Fig. 11 which is constructed from graph Γ based on triangular lattice. In Fig. 13a the highlighted qubits on which we correct the Z -errors are mapped to two copies of a surface code formed by triangles. The triangles in Fig. 13a are resized, the orientations are changed and redrawn as in the Fig. 13b. The triangles in Fig. 13b represent a surface code which can also be represented as shown in Fig. 13b by the dark colored edges which is the dual graph of Γ .

C. A structural result

Before, we end this section, we prove a structural result on the hypergraph subsystem codes obtained by a variation on Construction 3. Recall that in this construction the rank-3 edges are not in the boundaries of the e -faces. We consider a variation where the rank-3 edges are in the boundary of e -faces. These codes are not good in the sense of having a good distance, but they give an insight into some of the structures that must be avoided in order to obtain good hypergraph subsystem codes.

Theorem 20. *Consider a subsystem code obtained via Construction 3, where in step 3 the hyperedges are inserted on the e -faces of the 2-colex. Then the resulting subsystem code has $O(1)$ distance independent of the length of the code.*

Algorithm 4: Decoding generalized five-squares subsystem codes

Input: A generalized five squares substem color code on a hypergraph \mathcal{H}_Γ , where Γ is the bicolored graph used to construct \mathcal{H}_Γ via Construction 3.

Output: Error estimate \hat{E} .

```

1:  $\hat{E} = I$ 
2: for each  $e$ -face and  $f$ -face of  $\mathcal{H}_\Gamma$  do ▷ Correct  $X$  errors locally
3:   Measure rank-2 stabilizer of the face ie stabilizer of type S4 or S5. Let the syndrome be  $s$ 
4:    $\hat{E} = \hat{E} X_v^s$ 
5: end for
6: for each  $f \in v$ -face of  $\mathcal{H}_\Gamma$  do ▷ Correct some  $Z$  errors locally
7:   Measure rank-3 stabilizer of the face ie stabilizer of type S2. Let the syndrome be  $s$ .
8:    $\hat{E} = \hat{E} Z_v$  for some  $v \in f$ .
9: end for
10: for for  $f$  in  $f$ -faces of  $\mathcal{H}_\Gamma$  do ▷ Correct remaining  $Z$  errors globally
11:   Measure S1 and S3 stabilizer.
12: end for
13: Project the S1 syndromes of  $f \in F_a$  and S3 syndromes of  $f \in F_b$  on one copy of  $\Gamma^*$ .
14: Project the S3 syndromes of  $f \in F_a$  and S1 syndromes of  $f \in F_b$  on one copy of  $\Gamma^*$ .
15: Decode the errors on each copy of  $\Gamma$  using any 2D surface code decoder. Denote by  $E_1, E_2$  the estimates on each of
    copies.
16: Each qubit on the surface codes corresponds to a unique qubit on the  $\mathcal{H}_\Gamma$ . Denote this set of qubits by  $\Omega = \text{supp}(E_1) \cup$ 
     $\text{supp}(E_2)$ .
17: Return  $\hat{E} = \hat{E} \prod_{v \in \Omega} Z_v$ 

```

Proof. The hypergraph from this construction contains unit cells of the form shown in Figure 14.

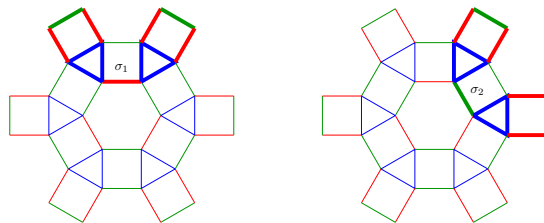


Fig. 14: (Color online) Examples of logical operators with $O(1)$ weight independent of the size of the code.

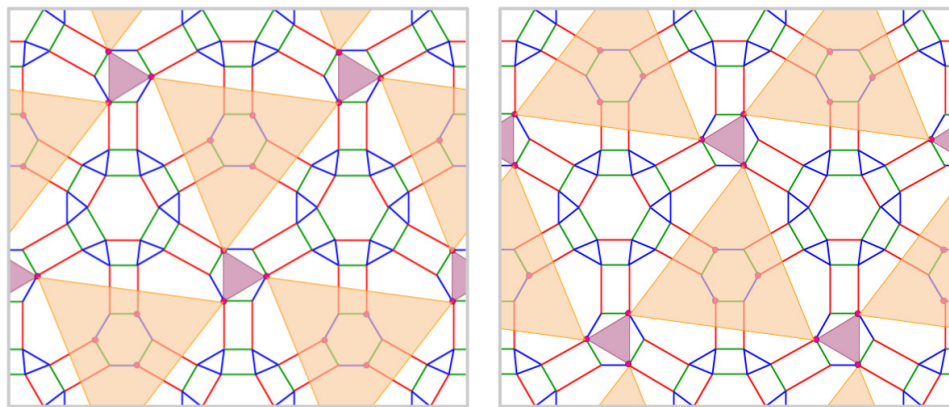
We can easily check that this hypergraph supports a hypercycle consisting of two neighboring hyperedges and the adjacent e -faces along with a rank-2 edge connecting the hyperedges. (Every vertex in the support of these edges has degree two with respect to these edges.) The associated loop operator $W(\sigma)$ is in the centralizer of the gauge group. Observe that we can also pair a hyperedge with another neighboring hyperedge to give another hypercycle. It can be easily verified that the operators associated to these two hypercycles anticommute. Therefore they cannot be in the center of the gauge group and hence there are not stabilizers of the subsystem code. In other words they are logical operators with a finite weight. Thus the distance of the code is $O(1)$. \square

In the preceding theorem we assume that the code is sufficiently big enough to contain structures of the form shown in Fig. 14. Although we only showed that these structures are to be avoided in the context of Construction 3, these structures should be avoided in any hypergraph subsystem code.

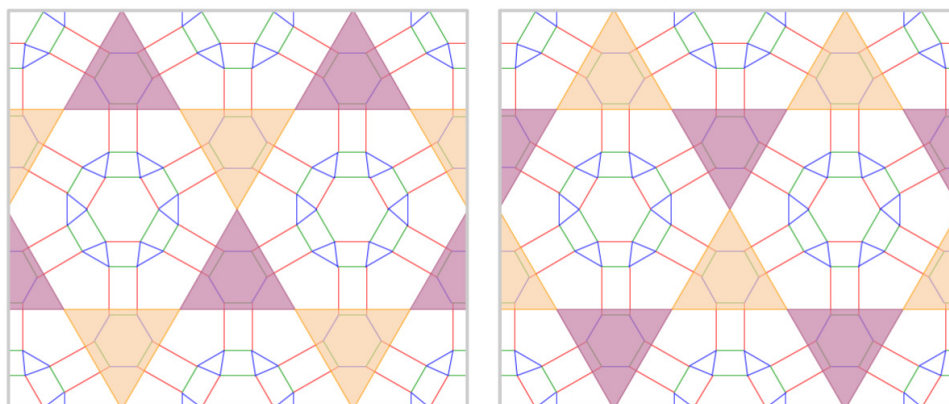
VI. SUBSYSTEM SURFACE CODES

The subsystem codes studied so far have been based on hypergraphs where the gauge group was generated by two body operators. In this section we study subsystem codes based on surfaces. These codes were proposed in [13]. In these codes the gauge group is generated by weight three generators. These codes are amenable for a planar implementation and enable fault tolerant quantum computation through code deformation techniques unlike the hypergraph subsystem codes which do not allow for code deformation through introduction of boundaries.

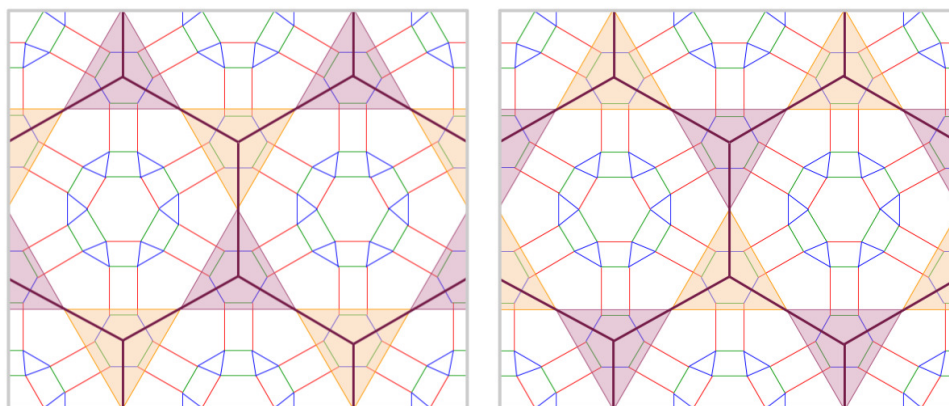
Recently, a new topological subsystem code based on a surface code was proposed by Bravyi et al. These codes have 3-qubit gauge operators and they enable fault tolerant quantum computing through code deformation techniques, a feature that was



(a) Mapping to two surface codes



(b) Redrawing the surface codes



(c) Representing each qubit by an edge instead of vertex will result in a surface code based on Γ^* as shown in this figure by the maroon colored solid edges

Fig. 13: (Color online) Example of mapping the generalized five-squares subsystem code to two surface codes constructed from the dual graph of Γ

absent in the previously known classes of subsystem codes. We generalize this construction to a large class of surface codes. Consequently, we are able to obtain a code which has a lower overhead compared to the codes [27].

A. Constructions of subsystem surface codes

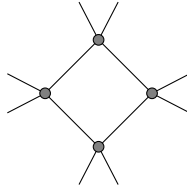
In this section we propose a general method to construct subsystem surface codes. Our method enables us to construct codes of lower overhead.

Construction 4: Generalized subsystem surface codes

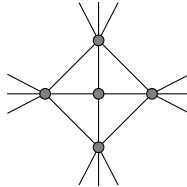
Input: A 4-valent graph Γ embedded on a surface such that all faces are even.

Output: A subsystem surface code on a graph \mathcal{H} .

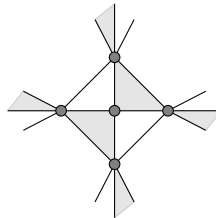
- 1: Find the medial graph of Γ . Denote it by Γ_m . Each 4-valent vertex gives rise to a new face. Let us call such a face a v -face.



- 2: In each v -face, add a new vertex and connect it to all the vertices in the face. Denote this as \mathcal{H}_Γ .



- 3: Color the resulting complex such that the f -faces are all of the same color and the triangles in the faces are 2-colorable.



- 4: Assign a gauge operator $Z_u Z_v Z_w$ or $X_u X_v X_w$ depending on the color of the triangular face.

- 5: Let $\mathcal{G} = \langle g_e \mid e \text{ is a triangle in } \mathcal{H}_\Gamma \rangle$.
-

Theorem 21. Let Γ be a 4-valent graph embedded on closed surface of genus g such that every face is even sided. Then Construction 4 gives a subsystem surface code encoding $2g$ qubits into $3v$ qubits, where $v = |V(\Gamma)|$ and g is the genus of surface. The code has $v - 2g - 2$ gauge qubits.

Proof. The number of vertices present in the medial graph Γ_m is equal to the number of edges present in Γ which is equal to $2v$ owing to the 4-valent nature of Γ . In addition, after Construction 4, v vertices are added. So the total number of qubits in the resulting subsystem surface code is $3v$.

The construction introduces four gauge operators for each vertex in Γ . Hence we have $4v$ gauge operators. Since the product of all the X or Z type gauge operators is identity, we have $4v - 2$ are independent generators for the gauge group.

From each face of Γ , we obtain two stabilizers s_f^X and s_f^Z , where

$$s_f^\sigma = \prod_{e \in \partial f} g_e^\sigma \quad (20)$$

where ∂f , is the boundary of f . Since s_f^σ is generated by the gauge operators, it is in the gauge group. We can also check that s_f^σ commutes with all the gauge operators and therefore it is in $C(\mathcal{G})$. It is evident that s_f^σ commutes with the gauge operators of the same type ie g_e^σ . Suppose $g_e^{\sigma'}$ is such that $\sigma \neq \sigma'$. If $e \in \partial f$, then $g_e^{\sigma'}$ and s_f^σ overlap in exactly two vertices and they commute. If $e \notin \partial f$, then it must overlap with s_f^σ in at most two vertices. If it overlaps in two or zero locations, then again they commute. Gauge operators g_e which overlap exactly once with s_f^σ must be in \mathcal{G}_σ , and hence commute. Observe that

$$\prod_f s_f^\sigma = I. \quad (21)$$

Thus, the number of independent stabilizer generators is $2(f - 1)$ where f is the number of faces in Γ . But in Γ , $v - 2v + f = 2 - 2g$ and therefore $f = 2 + v - 2g$. So the number of independent stabilizer generators is $s = 2(v - 2g + 1)$. If r is the number of gauge qubits, $2r = 4v - 2 - 2(v - 2g + 1)$ which gives $r = v + 2g - 2$. The dimension of the subsystem code is $k = n - s - r = 2g$. \square

Note that the faces of Γ_m correspond to the vertices and faces of Γ . A face in Γ_m which is derived from a face (vertex) in Γ is called an f -face (v -face). In \mathcal{H}_Γ , the triangles come from the v -faces of Γ_m and each v -faces gives rise to four such

triangles. Of more importance are the faces in \mathcal{H}_Γ which are derived from the f -faces of Γ_m . We shall call these faces of \mathcal{H}_Γ also as f -faces. Each of these correspond to faces in Γ so without ambiguity we can label them by the faces in Γ .

If $\chi = 2 - 2g$, the dimension of the code is $2 - \chi$ and the number of gauge qubits is $v - \chi$. Note that Γ gives a $[[2v, 2g]]$ surface code. The subsystem code adds 50% overhead. The natural question is if we can lower these overheads. On the torus, Kitaev's toric code on the square lattice has the parameters $[[2n^2, 2]]$. This code can be improved to give lower overheads, see [11]. Motivated by this construction we propose a class of subsystem surface codes that have lower overheads. We consider a different tiling of the torus proposed in [11], see Fig. 15. We observe that this graph meets the conditions of Construction 4 is applicable. Then by Theorem 21, we can obtain a $[[3(d^2 + 1)/2, 2, (d^2 + 1)/2, d]]$ subsystem code. With respect to the $[[3d^2, 2, d^2, d]]$ subsystem codes of Bravyi et al., they offer a reduced overhead. We conjecture that these are optimal.

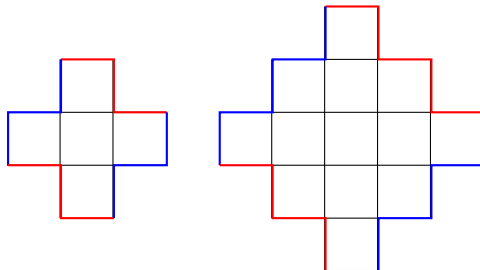


Fig. 15: (Color online) A $[[d^2 + 1, 2, d]]$ surface code on a torus for $d = 3, 5$. Boundaries of same color are to be identified.

B. Decoding subsystem surface codes

Theorem 22. *The subsystem surface codes of Theorem 21 can be efficiently decoded using Algorithm 5.*

Proof. As can be seen from the proof of Theorem 21, there are two types of stabilizers. Since they are either X -type or Z -type we can correct the bit flip and phase flip errors separately. Suppose we have a bit flip error on a qubit in the boundary of an f -face, such as qubit v in line 2 of Algorithm 5. This leads non zero syndrome for exactly two stabilizer generators $s_{f_1}^Z$ and $s_{f_2}^Z$. Similarly, bit flip errors on qubits w , cause nonzero syndrome for $s_{f_2}^Z$ and $s_{f_3}^Z$, X_s causes nonzero syndrome on $s_{f_3}^Z$ and $s_{f_4}^Z$ and X_t on $s_{f_1}^Z$ and $s_{f_3}^Z$. A bit flip error on the qubit in the interior of a v -face, such as u causes nonzero syndrome with respect to the $s_{f_2}^Z$ and $s_{f_4}^Z$. Note that the stabilizers $s_{f_1}^Z$ and $s_{f_2}^Z$ do not have any overlap with X_u and are unaffected. We can capture all this information by representing i) each f -face by a vertex ii) each qubit by a edge and iii) associate the stabilizer s_f^Z to the corresponding vertex, as shown in line 2 of Algorithm 5. With this mapping we can project the syndromes on the subsystem surface code to the vertices of Γ_X . We can then decode the errors on the surface code and lift it back to the subsystem code because there is a one to one correspondence between the errors on the surface code and the subsystem code. This allows us to lift the errors from the surface code to the subsystem code unambiguously. A similar reasoning for phase flip errors leads to the mapping shown in line 3. We omit the details. \square

VII. SIMULATION RESULTS

We have performed simulations for decoding the subsystem codes obtained from vertex expansion of color codes on square octagon lattice, for lattices of different sizes and for different depolarizing error rates. We generate a large number of error samples for each error rate and each lattice. For each error sample E , we then find an error estimate \hat{E} using one of our decoding algorithms, (specifically Algorithm 3). If the effective error $E_{eff} = E\hat{E}$ anti-commutes with any of the logical operators of the code, then we increment the number of failed decoding attempts. Thus obtaining the probability of failure for different error rates, we plot probability of failure against the depolarizing noise rate for lattices of different sizes.

We simulated for depolarizing noise rates ranging from 0 to 0.029 with a step size of 0.002 and for lattices with 192, 768 and 3072 qubits. For each data point 2500 samples were considered. Fig. 16 shows the result of the simulation. We obtained a noise threshold of about 1.75% for the algorithm using the two step decoding algorithm. involving the cleaning up of X -errors on each unit cell. This is comparable to the threshold of 2% obtained in [9]. Since our algorithms do not exploit the correlations between the X and Z errors, it is possible to improve our decoders. For the five squares code Bravyi et al. [27] obtained a noise threshold of about 2%.

VIII. CONCLUSION

Fault tolerant systems are a necessity without which no quantum computing systems can become a reality. Quantum codes are essential for quantum fault tolerance. For a quantum code to be useful it is important to have a low complexity decoder. Since subsystem codes require only two or three qubit measurements they could be more amenable for experimental realizations.

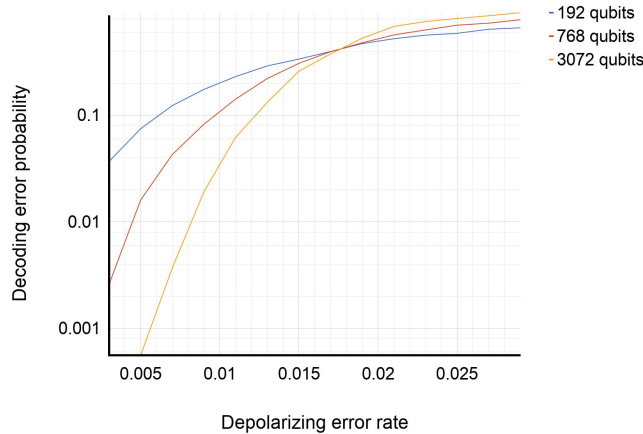


Fig. 16: Performance of the two step decoding algorithm for the hypergraph subsystem code on the square octagon lattice. Noise threshold is about 1.75%.

In our work, we have proposed algorithms for decoding different families of subsystem codes such as cubic subsystem color codes, topological subsystem color codes, hypergraph subsystem codes and subsystem surface codes. These decoding algorithms are applicable to a large classes of codes without requiring individual optimization for each code. We have shown how to decode cubic subsystem color codes by mapping them onto a surface code after a preprocessing step. Similarly subsystem surface codes can be decoded by mapping onto other topological codes such as color codes and surface codes. The advantage of this approach is that there are well established algorithms for decoding surface and color codes. We evaluated our decoding algorithms by numerical simulations and show that they achieve performance comparable to previously known decoders.

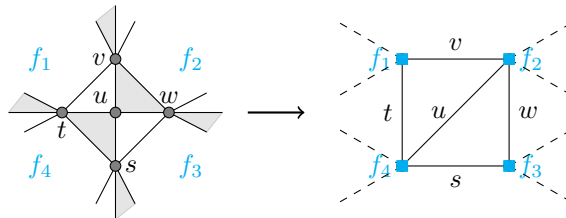
In addition we showed some structural results on subsystem codes which are of independent interest. We showed that certain classes of hypergraph subsystem codes have poor distance. These results hint that some configurations to be avoided for good hypergraph subsystem codes. We also gave a new construction for subsystem surface codes. This gave a family of subsystem

Algorithm 5: Decoding subsystem surface code

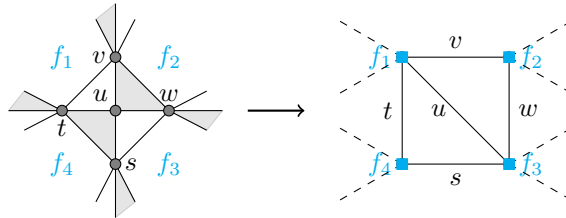
Input: A subsystem surface code on \mathcal{H}_Γ constructed from a graph Γ according to Construction 4 and syndromes $s_f^i, f \in F(\Gamma)$ and $i \in \{X, Z\}$.

Output: Error estimate \hat{E} such that \hat{E} has the input syndrome.

- 1: $\hat{E} = I$
- 2: Construct Γ_X with vertices labeled by f -faces of \mathcal{H}_Γ as shown below.



- 3: Construct Γ_Z with vertices labeled by f -faces of \mathcal{H}_Γ as shown below.



- 4: Project syndromes s_f^X and s_f^Z onto vertices of Γ_X and Γ_Z for all $f \in F(\Gamma)$ where Γ_X and Γ_Z are constructed from \mathcal{H}_Γ as above.
 - 5: Decode the errors on Γ_X and Γ_Z using any 2D surface code decoder. Denote by E'_X and E'_Z , the estimates.
 - 6: Lift the errors E'_X, E'_Z to subsystem code. Denote them \bar{E}_X and \bar{E}_Z respectively.
 - 7: Return $\hat{E} = \bar{E}_X \bar{E}_Z$
-

surface codes with lower overheads.

APPENDIX

We give an example of the construction of subsystem codes from Construction 2 in Fig. 17. The 2-colex is obtained in this figure is obtained from Construction 1. The assignment of the gauge operators differs from a subsystem code obtained from vertex expansion, see Fig. 5.

The resulting subsystem code has four types of stabilizers. These are shown in Fig. 18.

- (i) A cycle consisting of simple edges surrounding an f -face of Γ_2 .
- (ii) A cycle formed by alternating simple and hyperedges on the outer boundary of a v -face and alternating simple edges on the boundary of its inner face introduced by construction 2.
- (iii) A cycle consisting of alternating simple edges around an f -face and the simple and hyperedges belonging to the surrounding v - and f - faces.
- (iv) A loop of simple edges forming the inner face of a v -face.

As in Algorithm 3, the bit flip errors are corrected first using the stabilizers from rank-2 cycles. This leaves Z errors on the hyperedges. To correct the phase flip errors, the subsystem code is then mapped to the color code based on square octagon lattice as shown in Fig. 19 underlying the subsystem code. The error estimated after decoding the color code is then lifted to the subsystem code. For every Z error estimated in the color code the corresponding error estimate on the subsystem code will be the Z errors on the three qubits of the corresponding hyperedge.

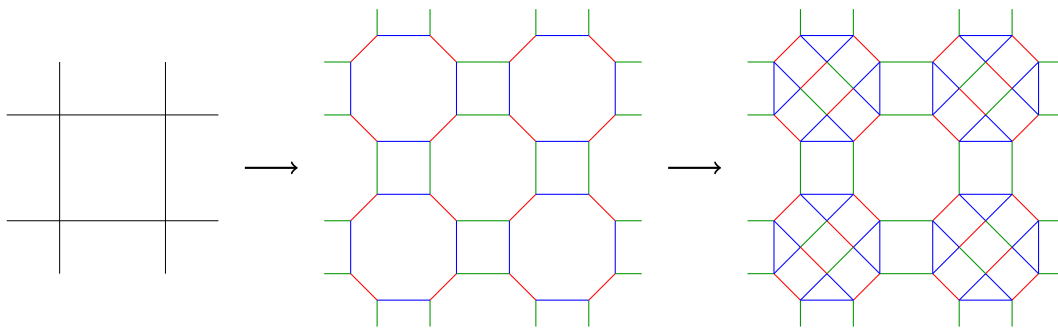
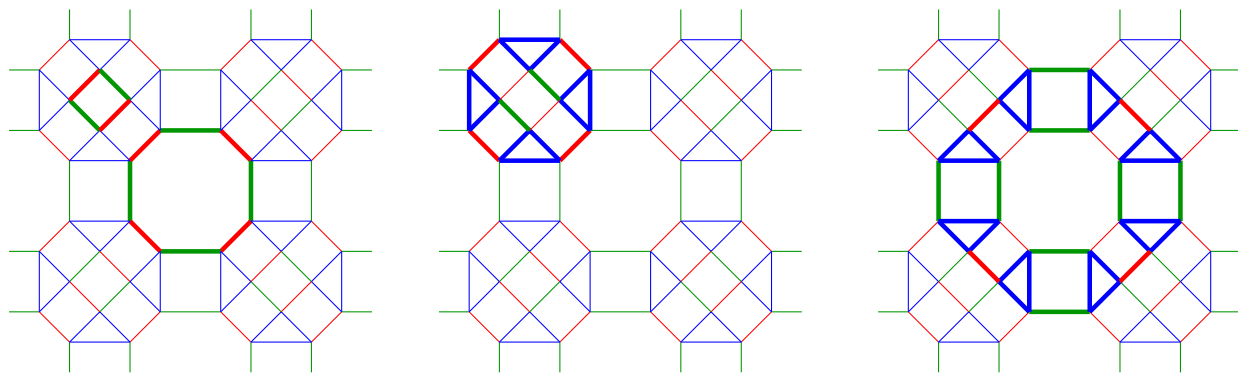


Fig. 17: Construction of uniform rank-3 hypergraph subsystem codes based on square lattice: A 2-colex is constructed from the square lattice using Construction 1. The subsystem code is constructed from the 2-colex using Construction 2



(a) The cycles formed by thick edges show the simple cycles around respective faces

(b) The thick simple edges and thick hyper edges constitute a hyper cycle around the square face

(c) The hyperedges highlighted with thick blue edges and thick simple edges form a hypercycle around the octagon face

Fig. 18: (Color online) Illustrating two types of cycles associated with the stabilizers of uniform rank-3 hypergraph subsystem codes constructed from square lattice.

ACKNOWLEDGMENT

The authors would like to thank Amit Anil Kulkarni for assistance with the simulations. PS would like to thank David Poulin for helpful discussions on subsystem codes.

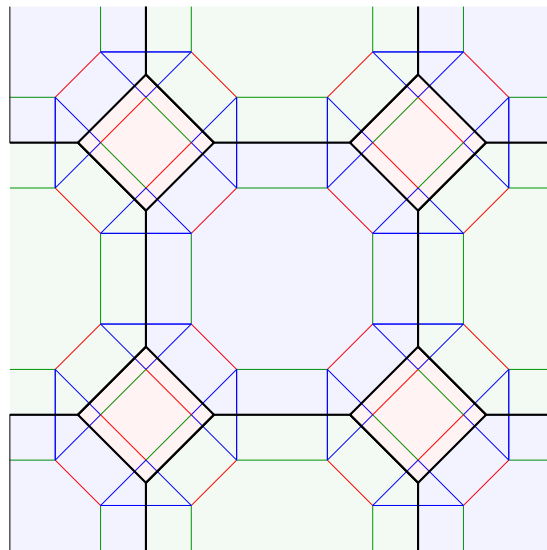


Fig. 19: (Color online) Mapping the uniform rank-3 hypergraph constructed in Fig. 17 to a 2-colex, by contracting the rank-3 edges and removing parallel edges.

REFERENCES

- [1] P. Aliferis and A. W. Cross. Sub-system fault tolerance with the bacon-shor code. *Phys. Rev. Lett.*, 98(220502), 2007.
- [2] A. Alosious, A. Bhagoji, and P. K. Sarvepalli. On the local equivalence of 2d color codes and surface codes with applications. *arXiv:quant-ph/1804.00866*, apr 2017.
- [3] Salah A. Aly, A. Klappenecker, and P. K. Sarvepalli. Subsystem codes. *44th Annual Allerton Conference on Communication, Control, and Computing*, 2006.
- [4] D. Bacon. Operator quantum error correcting subsystems for self-correcting quantum memories. *Phys. Rev. A*, 73(012340), 2006.
- [5] D. Bacon and A. Casaccino. Quantum error correcting subsystem codes from two classical linear codes. *44th Annual Allerton Conference on Communication, Control, and Computing*, 2006.
- [6] A. Bhagoji and P. K. Sarvepalli. Equivalence of 2d color codes (without translational symmetry) to surface codes. *IEEE International Symposium on Information Theory (ISIT)*, 2015, jun 2015.
- [7] H. Bombin. Topological subsystem codes. *Phys. Rev. Lett.*, 81(032301), 2010.
- [8] H. Bombin. An introduction to topological quantum codes. In Daniel A. Lidar and Todd A. Brun, editors, *Quantum Error Correction*, chapter Topological Codes, pages 1–35. Cambridge University Press, New York, 2013.
- [9] H. Bombin, G. Duclos-Cianci, and D. Poulin. Universal topological phase of two-dimensional stabilizer codes. *New Journal of Physics*, 14(7):073048, 2012.
- [10] H. Bombin and M. A. Martin-Delgado. Topological quantum distillation. *Physical Review Letters*, 97(18), 2006.
- [11] H. Bombin and M. A. Martin-Delgado. Topological quantum error correction with optimal encoding rate. *Phys. Rev. A*, 73:062303, Jun 2006.
- [12] H. Bombin and M. A. Martin-Delgado. Exact topological quantum order in d=3 and beyond: Branyons and brane-net condensates. *Phys. Rev. B*, Feb 2007.
- [13] S. Bravyi, G. Duclos-Cianci, D. Poulin, and M. Suchara. Subsystem surface codes with three-qubit check operators. *Quant. Inf. Comp.*, 13:963–985, 2013.
- [14] A. R. Calderbank, E. M. Rains, P.W. Shor, and N. J. A. Sloane. Quantum error correction via codes over GF(4). *IEEE Trans. Inform. Theory*, 44:1369–1387, 1998.
- [15] N. Delfosse. Decoding color codes by projection onto surface codes. *Physical Review A - Atomic, Molecular, and Optical Physics*, 89:1–12, 2014.
- [16] D. Gottesman. A class of quantum error-correcting codes saturating the quantum Hamming bound. *Phys. Rev. A*, 54:1862–1868, 1996.
- [17] D. Gottesman. Stabilizer codes and quantum error correction. *arXiv:quant-ph/9705052*, 2008:114, 1997.
- [18] G. Kells, A. T. Bolukbasi, V. Lahtinen, J. K. Slingerland, J. K. Pachos, and J. Vala. Topological degeneracy and vortex manipulation in kitaev’s honeycomb model. *Phys. Rev. Lett.*, (3):1–4, 2008.
- [19] A. Kitaev. Fault-tolerant quantum computation by anyons. *Annals of Physics*, 303:2–30, 2003.
- [20] A. Kitaev. Anyons in an exactly solved model and beyond. *Annals of Physics*, 321(1):2–111, 2006.
- [21] A. Klappenecker and P. K. Sarvepalli. Clifford code constructions of operator quantum error-correcting codes. *IEEE Transactions on Information Theory*, 54(12):5760–5765, 2008.
- [22] D. W. Kribs, R. Laflamme, and D. Poulin. Unified and generalized approach to quantum error correction. *Phys. Rev. Lett.*, 94(180501), 2005.
- [23] D. W. Kribs, R. Laflamme, D. Poulin, and M. Lesosky. Operator quantum error correction. *Quant. Inf. & Comp.*, pages 383–399, 2006. Eprint: quant-ph/0504189.
- [24] Yi-Chan Lee, Courtney Brell, and Steven T. Flammia. Topological quantum error correction in the kitaev honeycomb model. *Journal of Statistical Mechanics: Theory and Experiment*, 2017.
- [25] D. Poulin. Stabilizer formalism for operator quantum error correction. *Phys. Rev. Lett.*, 95(230504), 2005.
- [26] P. K. Sarvepalli and K. R. Brown. Topological subsystem codes from graphs and hypergraphs. *Phys. Rev. A*, 86:042336, Oct 2012.
- [27] M. Suchara, S. Bravyi, and B. Terhal. Constructions and noise threshold of topological subsystem codes. *Journal of Physics A*, 3, 2011.
- [28] D. S. Wang, A. G. Fowler, C. D. Hill, and L. C. L. Hollenberg. Graphical algorithms and threshold error rates for the 2d colour code. *Quantum Information and Computation*, 10:780, 2010.